Available online at www.sciencedirect.com
SCIENCE DIRECT®
Journal of Magnetic Resonance 180 (2006) 39–50
JMR Journal of Magnetic Resonance
www.elsevier.com/locate/jmr

Optimum spin-state selection for all multiplicities in the acquisition dimension of the HSQC experiment

Pau Nolis [a], Juan Félix Espinosa [b], Teodor Parella [a,*]

[a] Servei de Ressonància Magnètica Nuclear, Universitat Autònoma de Barcelona, E-08193 Bellaterra, Barcelona, Spain
[b] Centro de Investigación Lilly, Avda. de la Industria 30, E-28108 Alcobendas, Spain

Received 22 November 2005; revised 29 December 2005
Available online 30 January 2006

Abstract

Most conventional heteronuclear spin-state-selective (S^3) NMR experiments only work for a specific multiplicity, typically IS spin systems. Here, we introduce a general and efficient IPAP strategy to achieve S^3 editing simultaneously for all multiplicities in the acquisition dimension of the HSQC experiment. Complementary in-phase (HSQC-IP) and anti-phase (HSQC-AP) data are separately recorded with a simple phase exchange of two 90° proton pulses involved in the mixing process of the F2-coupled sensitivity-improved HSQC pulse sequence. Additive and subtractive linear combination of these IP/AP data generates simplified F2-α/β-spin-edited HSQC subspectra for all IS, I_2S, and I_3S spin systems and combines enhanced and optimized sensitivity with excellent tolerance to unwanted cross-talk contributions over a considerable range of coupling constants. Practical aspects such as pulse phase settings, transfer efficiency dependence, inter-pulse delay optimization, and percentage of cross-talk are theoretically analyzed and discussed as a function of each I_nS multiplicity. Particular emphasis on the features associated to spin-editing in diastereotopic I_2S spin systems and application to the measurement of long-range proton–carbon coupling constants are also provided.
© 2006 Published by Elsevier Inc.

Keywords: NMR; HSQC; Spin-state selection; Coupling constants; Spin-editing

1. Introduction

The heteronuclear single-quantum correlation (HSQC) experiment is one of the most important tools for high-resolution NMR studies of molecules in solution. It is the basis of many different and very important multidimensional NMR experiments developed for the study of small-to-medium sized molecules at natural abundance and also for large isotopic labeled bio-molecules, in particular proteins and nucleic acids. Thus, any modification in the regular HSQC pulse scheme can have a great impact in the design of new and improved NMR methodologies because of the easy extrapolation on many different applications. Examples on the importance of some improvements introduced into the basic HSQC pulse sequence have been the incorporation of pulsed-field gradients for coherence selection combined with the PEP principle for sensitivity-improved versions [1,2], the use of water-flip back techniques for a proper application in bio-molecules dissolved in non-deuterated water, or the modification of the coherence-transfer mixing period to afford specific spin-state-selective (S^3) editing, as established in the widely known TROSY experiment [3]. The principles associated to homonuclear and heteronuclear spin-editing have emerged as an important feature in modern heteronuclear NMR spectroscopy in order to simplify spectra and to avoid peak overlapping and it has been widely used to measure scalar and residual dipolar couplings or to study the relaxation properties of the different lines belonging to the same multiplet. All S^3-based NMR experiments employ two different ways to perform the addition/subtraction procedure of the in-phase (IP) and anti-phase (AP) data: (i) design of a specific pulse train that combines coherently the two

* Corresponding author. Fax: +34 93 5812291.
E-mail address: teodor.parella@uab.es (T. Parella).

1090-7807/$ - see front matter © 2006 Published by Elsevier Inc.
doi:10.1016/j.jmr.2006.01.003

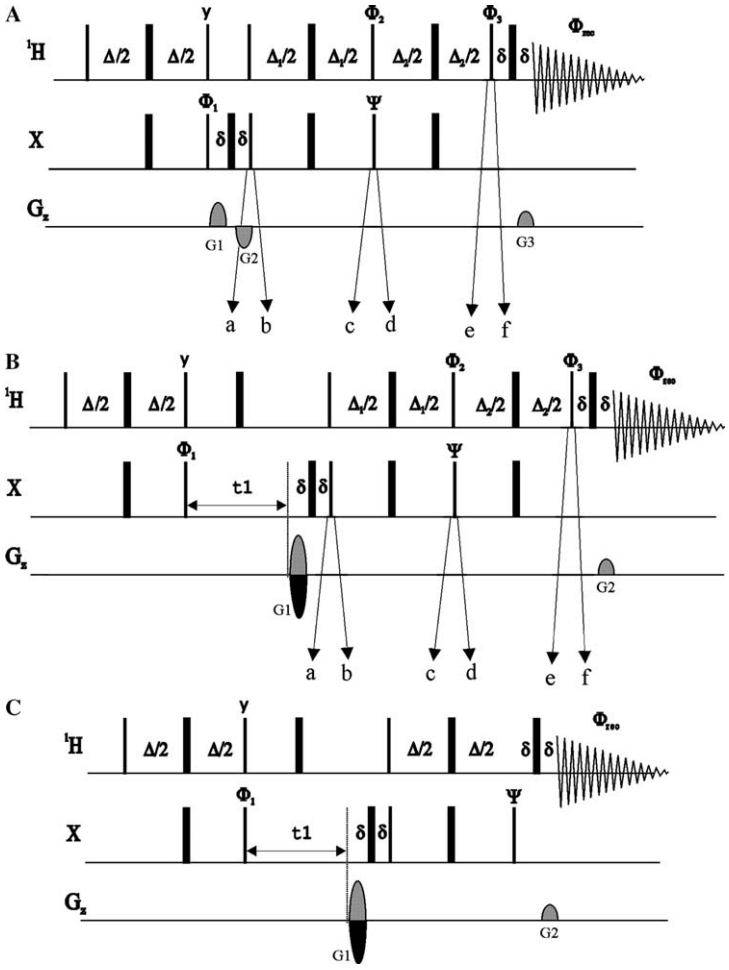

Fig. 1. Pulse sequences of the (A) 1D and (B) 2D versions of the F2-coupled ^{1}H–X sensitivity-improved HSQC experiment to achieve spin-selected spectra simultaneously for all IS, I_2S, and I_3S spin systems: (i) HSQC-IP(y): ($\phi_2 = y$, $\varphi_3 = x$, $\Psi = y$); (ii) HSQC-AP(y): ($\phi_2 = x$, $\varphi_3 = y$, $\Psi = y$); (iii) HSQC-IP(x): ($\phi_2 = y$, $\varphi_3 = x$, $\Psi = x$); (iv) HSQC-AP(x): ($\phi_2 = x$, $\varphi_3 = y$, $\Psi = x$). (C) Original HSQC-α/β pulse train, as reported in [4–7] ($\Psi = y$) and in [24] ($\Psi = x$). Thick and thin rectangles represent 90° and 180° pulses, respectively. A basic two-step phase cycle was used ($\phi_1 = \phi_{rec} = x, -x$). The delay Δ is optimized to $1/2J$(IS) whereas Δ_1 and Δ_2 are optimized as a function of the experiment and multiplicity (see Table 4 for details). See Tables 1–3 for magnetization components available at times a–f.

observable IP and AP magnetization components prior to data acquisition, or (ii) separate recording of the IP and AP components using equivalent pulse schemes followed by a post-processing mathematical protocol. In principle, this second approach should be much more attractive from the sensitivity point of view because if two spectra are added prior to acquisition, one component is lost, while both are retained when post-acquisition editing is used.

Nowadays, heteronuclear spin-editing in 2D HSQC spectra can be achieved in the directly detected F2-dimension (referred as HSQC-α/β experiment) [4–7], in the indirect F1-dimension (α/β-HSQC or also known as IPAP-HSQC experiment) [8], or in both dimensions by E.COSY- or TROSY-type selection in F1,F2-coupled HSQC experiments (α/β-HSQC-α/β) [3,9,10]. These reported S^3-edited HSQC experiments only work properly for IS spin systems and they have been mainly applied to backbone NH and $C_\alpha H_\alpha$ spin systems in labeled proteins. During the last years, a different number of methylene-specific [11–16] and methyl-specific [17–20] spin-edited HSQC-type pulse

Table 1
Product operator components of a IS spin system present at different times of the HSQC experiment (Fig. 1B) following the evolution time t_1[b,c]

Phases	t_1[a]	b	c	d	e	f
$\phi_2 = y$	$H_zS_x\cos(\Omega_S t_1)$	H_yS_x	H_yS_x	H_yS_z	H_xs'	$\mathbf{H_xs'}$
$\phi_3 = x$	$H_zS_y\sin(\Omega_S t_1)$	H_yS_z	H_xs	H_zs	H_zs	$\mathbf{H_ys}$
$\Psi = y$						
$\phi_2 = x$	$H_zS_x\cos(\Omega_S t_1)$	H_yS_x	H_yS_x	H_zS_z	H_zS_z	$\mathbf{H_xS_z}$
$\phi_3 = y$	$H_zS_y\sin(\Omega_S t_1)$	H_yS_z	H_xs	H_xs	H_yS_zss'	$\mathbf{H_yS_zss'}$
$\Psi = y$						
$\phi_2 = y$	$H_zS_x\cos(\Omega_S t_1)$	H_yS_x	H_yS_x	H_yS_x	H_yS_x	H_yS_x
$\phi_3 = x$	$H_zS_y\sin(\Omega_S t_1)$	H_yS_z	H_xs	H_zs	H_zs	$\mathbf{H_ys}$
$\Psi = x$						
$\phi_2 = x$	$H_zS_x\cos(\Omega_S t_1)$	H_yS_x	H_yS_x	H_zS_x	S_ys'	S_ys'
$\phi_3 = y$	$H_zS_y\sin(\Omega_S t_1)$	H_yS_z	H_xs	H_xs	H_yS_zss'	$\mathbf{H_yS_zss'}$
$\Psi = x$						

[a] Trigonometric factors showing chemical shift dependence are shown only on this column.
[b] $\Delta = 1/(2J)$.
[c] Trigonometric simplifications: $s = \sin(\pi J_{HS}\Delta_1)$; $c = \cos(\pi J_{HS}\Delta_1)$; $s' = \sin(\pi J_{HS}\Delta_2)$; $c' = \cos(\pi J_{HS}\Delta_2)$.

schemes have been designed and analyzed in terms of sensitivity and spin-editing. In a recent paper, heteronuclear cross-polarization (HCP) has been demonstrated to be a useful mixing element in heteronuclear correlation experiments to achieve different spin-selection patterns simultaneously for IS and I_2S spin systems [21].

In this work, we describe an improved way to obtain spin-editing in HSQC-α/β spectra. This experiment has been previously reported for the measurement of several homo- and heteronuclear coupling constants in small and medium-sized natural-abundance molecules and also in labeled proteins [4–7,22–26] or to increase the sensitivity in carbon-detected 2D and 3D HACACO-α/β experiments [27,28]. We show that a phase exchange of some 90° proton pulses involved in the coherence-order-selective (COS) coherence-transfer (CT) mixing process of a F2-coupled sensitivity-improved HSQC experiment can afford a separate and fully complementary AP magnetization component to the traditional IP one. After additive/subtractive linear combination, heteronuclear spin-editing in the acquisition dimension is achieved for IS spin systems as described previously in the HSQC-α/β experiment [4–7]. In addition, our scheme offers two important benefits: (i) spin-editing is also achieved for other I_nS multiplicities and, (ii) its sensitivity is optimized using the same principles as known for the sensitivity-improved HSQC experiment [2]. We examine our method theoretically, by using the product-operator formalism, and by spectra simulation and also experimentally. Experimental verification is illustrated for CH, CH_2, and CH_3 spin systems in molecules

Table 2
Product operator components of a I_1I_2S spin system present at different times of the HSQC experiment (Fig. 1B) following the evolution time t_1[b,c]

Phases	t_1[a]	b	c	d	e	f
$\phi_2 = y$	$H_{1z}S_x\cos(\Omega_S t_1)$	$H_{1y}S_x$	$H_{1y}S_xc$	$H_{1y}S_zc$	$H_{1x}cs'$	$\mathbf{H_{1x}cs'}$
$\phi_3 = x$	$H_{1z}S_y\sin(\Omega_S t_1)$	$H_{1y}S_z$	$H_{1y}H_{2z}S_ys$	$H_{1y}H_{2x}S_ys$	$H_{1y}H_{2x}S_ys$	$H_{1z}H_{2x}S_ys$
$\Psi = y$			$H_{1x}s$	$H_{1z}s$	$H_{1z}s$	$\mathbf{H_{1y}s}$
$\phi_2 = x$	$H_{1z}S_x\cos(\Omega_S t_1)$	$H_{1y}S_x$	$H_{1y}S_xc$	$H_{1z}S_zc$	$H_{1z}S_zc$	$\mathbf{H_{1x}S_zc}$
$\phi_3 = y$	$H_{1z}S_y\sin(\Omega_S t_1)$	$H_{1y}S_z$	$H_{1y}H_{2z}S_ys$	$H_{1z}H_{2y}S_ys$	$H_{2y}S_xss'$	$H_{2y}S_xs's$
$\Psi = y$			$H_{1x}s$	$H_{1x}s$	$H_{1y}S_zss$	$\mathbf{H_{1y}S_zss'}$
$\phi_2 = y$	$H_{1z}S_x\cos(\Omega_S t_1)$	$H_{1y}S_x$	$H_{1y}S_xc$	$H_{1y}H_{2x}S_zs$	$H_{1y}H_{2x}S_zsc'^2$	$\mathbf{H_{1z}H_{2x}S_zsc'^2}$
$\phi_3 = x$	$H_{1z}S_y\sin(\Omega_S t_1)$	$H_{1y}S_z$	$H_{1y}H_{2z}S_ys$	$H_{1z}s$	$H_{1x}H_{2y}S_zss'^2$	$\mathbf{H_{1x}H_{2z}S_zss'^2}$
$\Psi = x$			$H_{1x}s$		$H_{1z}s$	$\mathbf{H_{1y}s}$
$\phi_2 = x$	$H_{1z}S_x\cos(\Omega_S t_1)$	$H_{1y}S_x$	$H_{1y}S_xc$	$H_{1z}H_{2y}S_zs$	$H_{1z}H_{2x}ss'$	$\mathbf{H_{1x}H_{2z}s's}$
$\phi_3 = y$	$H_{1z}S_y\sin(\Omega_S t_1)$	$H_{1y}S_z$	$H_{1y}H_{2z}S_ys$	$H_{1x}s$	$H_{1y}S_zss'$	$\mathbf{H_{1y}S_zs's}$
$\Psi = x$			$H_{1x}s$			

[a] Trigonometric factors showing chemical shift dependence are shown only on this column.
[b] $\Delta = 1/(2J)$.
[c] Trigonometric simplifications: $s = \sin(\pi J_{HS}\Delta_1)$; $c = \cos(\pi J_{HS}\Delta_1)$; $s' = \sin(\pi J_{HS}\Delta_2)$; $c' = \cos(\pi J_{HS}\Delta_2)$.

Table 3
Product operator components of a $I_1I_2I_3S$ spin system present at different times of the HSQC experiment (Fig. 1B) following the evolution time t_1[b,c]

Phases	t_1[a]	b	c	d	e	f[d]
$\phi_2 = y$	$H_{1z}S_x\cos(\Omega_S t_1)$	$H_{1y}S_x$	$H_{1y}S_xc^2$	$H_{1y}S_zc^2$	$H_{1x}c^2s'$	$\mathbf{H_{1x}c^2s'}$
$\phi_3 = x$	$H_{1z}S_y\sin(\Omega_S t_1)$	$H_{1y}S_z$	$H_{1y}H_{2z}H_{3z}S_xs^2$	$H_{1y}H_{2x}H_{3x}S_zs^2$	$H_{1y}H_{2x}H_{3y}s^2c'^2s'$	$\mathbf{H_{1z}H_{2x}H_{3z}s^2c'^2s'}$
$\Psi = y$			$H_{1x}s$	$H_{1z}s$	$H_{1y}H_{2y}H_{3x}s^2c'^2s'$	$\mathbf{H_{1z}H_{2z}H_{3x}s^2c'^2s'}$
					$H_{1y}H_{2y}H_{3x}S_zs^2c's'^2$	$\mathbf{H_{1z}H_{2z}H_{3x}S_zs^2c's'^2}$
					$H_{1x}H_{2y}H_{3y}s^2s'^3$	$\mathbf{H_{1x}H_{2z}H_{3z}s^2s'^3}$
					$H_{1z}s$	$\mathbf{H_{1y}s}$
$\phi_2 = x$	$H_{1z}S_x\cos(\Omega_S t_1)$	$H_{1y}S_x$	$H_{1y}S_xc^2$	$H_{1z}S_zc^2$	$H_{1z}S_zc^2$	$\mathbf{H_{1x}S_zc^2}$
$\phi_3 = y$	$H_{1z}S_y\sin(\Omega_S t_1)$	$H_{1y}S_z$	$H_{1y}H_{2z}H_{3z}S_xs^2$	$H_{1z}H_{2y}H_{3y}S_zs^2$	$H_{1z}H_{2x}H_{3x}S_zs^2s'^2$	$\mathbf{H_{1x}H_{2z}H_{3z}S_zs^2s'^2}$
$\Psi = y$			$H_{1x}s$	$H_{1x}s$	$H_{1y}S_zss'$	$\mathbf{H_{1y}S_zs's}$
$\phi_2 = y$	$H_{1z}S_x\cos(\Omega_S t_1)$	$H_{1y}S_x$	$H_{1y}H_{2z}S_ysc$	$H_{1y}H_{2x}S_zsc$	$H_{1y}H_{2x}S_zscc'^2$	$\mathbf{H_{1z}H_{2y}S_zscc'^2}$
$\phi_3 = x$	$H_{1z}S_y\sin(\Omega_S t_1)$	$H_{1y}S_z$	$H_{1y}H_{3z}S_ysc$	$H_{1y}H_{3x}S_zsc$	$H_{1x}H_{2y}S_zscs'^2$	$\mathbf{H_{1x}H_{2z}S_zscs'^2}$
$\Psi = x$			$H_{1x}s$	$H_{1z}s$	$H_{1y}H_{3x}S_zscc'^2$	$\mathbf{H_{1z}H_{3x}S_zscc'^2}$
					$H_{1x}H_{3y}S_zscs'^2$	$\mathbf{H_{1x}H_{3z}S_zscs'^2}$
					$H_{1z}s$	$\mathbf{H_{1y}s}$
$\phi_2 = x$	$H_{1z}S_x\cos(\Omega_S t_1)$	$H_{1y}S_x$	$H_{1y}H_{2z}S_ysc$	$H_{1z}H_{2y}S_zsc$	$H_{1z}H_{2x}css'$	$\mathbf{H_{1x}H_{2z}css'}$
$\phi_3 = y$	$H_{1z}S_y\sin(\Omega_S t_1)$	$H_{1y}S_z$	$H_{1y}H_{3z}S_ysc$	$H_{1z}H_{3y}S_zsc$	$H_{1z}H_{3x}css'$	$\mathbf{H_{1x}H_{3z}css'}$
$\Psi = x$			$H_{1x}s$	$H_{1x}s$	$H_{1y}S_zss'$	$\mathbf{H_{1y}S_zs's}$

[a] Trigonometric factors showing chemical shift dependence are shown only on this column.
[b] $\Delta = 1/(2J)$.
[c] Trigonometric simplifications: $s = \sin(\pi J_{HS}\Delta_1)$; $c = \cos(\pi J_{HS}\Delta_1)$; $s' = \sin(\pi J_{HS}\Delta_2)$; $c' = \cos(\pi J_{HS}\Delta_2)$.
[d] Homonuclear anti-phase terms should be only observable for non-degenerate protons.

Table 4
Amplitude transfer and maximum relative intensity for IS, I_2S and I_3S spin systems in HSQC-IP and HSQC-AP experiments

NMR experiment	Phases	Amplitude transfer for I_nS spin system[a]	Maximum theoretical intensity[b]	Optimal delay settings
HSQC-IP(y)	$\phi_2 = y$; $\phi_3 = x$ $\Psi = y$	$s + s'c^{n-1}$	IS: 2 I_2S: 1.41 I_3S: 1.25	IS: $\Delta_1 = \Delta_2 = 1/2J$ I_2S: $\Delta_1 = 1/4J$; $\Delta_2 = 1/2J$ I_3S: $\Delta_1 = 1/6J$; $\Delta_2 = 1/2J$
HSQC-AP(y)	$\phi_2 = x$; $\phi_3 = y$ $\Psi = y$	$ss' + c^{n-1}$	IS: 2 I_2S: 1.41 I_3S: 1.25	IS: $\Delta_1 = \Delta_2 = 1/2J$ I_2S: $\Delta_1 = 1/4J$; $\Delta_2 = 1/2J$ I_3S: $\Delta_1 = 1/6J$; $\Delta_2 = 1/2J$
HSQC-IP(x)	$\phi_2 = y$; $\phi_3 = x$ $\Psi = x$	$s[1 + (n-1)c^{n-2}]$	IS: 1 I_2S: 2 I_3S: 1.76	IS: $\Delta_1 = 1/2J$; Δ_2[c] I_2S: $\Delta_1 = 1/2J$; Δ_2[c] I_3S: $\Delta_1 = 1/3{,}35J$; Δ_2[c]
HSQC-AP(x)	$\phi_2 = x$; $\phi_3 = y$ $\Psi = x$	$ss'[1 + (n-1)c^{n-2}]$	IS: 1 I_2S: 2 I_3S: 1.76	IS: $\Delta_1 = \Delta_2 = 1/2J$ I_2S: $\Delta_1 = \Delta_2 = 1/2J$ I_3S: $\Delta_1 = 1/3{,}35J$; $\Delta_2 = 1/2J$

[a] Trigonometric simplifications: $s = \sin(\pi J_{HS}\Delta_1)$; $c = \cos(\pi J_{HS}\Delta_1)$; $s' = \sin(\pi J_{HS}\Delta_2)$; $c' = \cos(\pi J_{HS}\Delta_2)$.
[b] Relative intensities compared to a conventional HSQC-IP experiment acquired at point c and a HSQC-AP experiment acquired at point b in Fig. 1B (normalized to 1 for all multiplicities).
[c] The Δ_2 delay is not necessary in the HSQC-IP(x) version. In practice, Δ_2 is optimized to $1/2J$ for any multiplicity in order that IP(x) data should be fully complementary to the equivalent AP(x) data.

at natural abundance and also for NH and NH_2 spin systems in labeled proteins. Examples will be provided for the measurement of long-range proton–carbon coupling constants and also for the single-line component selection in diastereotopic methylene resonances.

2. Results and discussion

The one-dimensional (1D) and two-dimensional (2D) pulse schemes used in this work (Fig. 1) are simple modifications of the sensitivity-enhanced HSQC experiment [1,2], with omission of the X-decoupling during ^{1}H acquisition. The 1D version (Fig. 1A) has been used to simulate the theoretical behavior of different I_nS ($n = 1$–3) spin systems. On the other hand, 2D experiments have been experimentally recorded using the pulse sequence of Fig. 1B and compared to the previously reported HSQC-α/β experiment (Fig. 1C) [4–7]. A detailed analysis of the different magnetization components present at different stages of the coherence-transfer mixing element (times a–f) for different IS, I_2S, and I_3S spin systems as a function of the phase of 90° I (ϕ_2, ϕ_3) and S (Ψ) pulses (Fig. 1) has been made and the results are summarized in Tables 1–3. Henceforth, experiments recorded with $\phi_2 = y$ and $\phi_3 = x$ will be termed HSQC-IP experiments whereas HSQC-AP will make reference to spectra obtained with $\phi_2 = x$ and $\phi_3 = y$. On the other hand, experiments recorded with $\Psi = y$ or $\Psi = x$ will be called HSQC(y) and HSQC(x), respectively. Thus, four combinations HSQC-IP(y), HSQC-AP(y), HSQC-IP(x), and HSQC-AP(x) are possible (Table 4). The conventional sensitivity-enhanced HSQC pulse sequence [1,2] is identical to the HSQC-IP(y) ($\phi_2 = y$, $\phi_3 = x$ and $\Psi = y$).

In principle, simultaneous S^3 editing for all multiplicities in the HSQC experiment could be achieved by combining separate IP and AP data. The AP component could be obtained by starting the acquisition just before the 90°(I,S) pulse following the variable evolution period (point b in Fig. 1) while the IP component after the refocusing period of the conventional HSQC pulse scheme

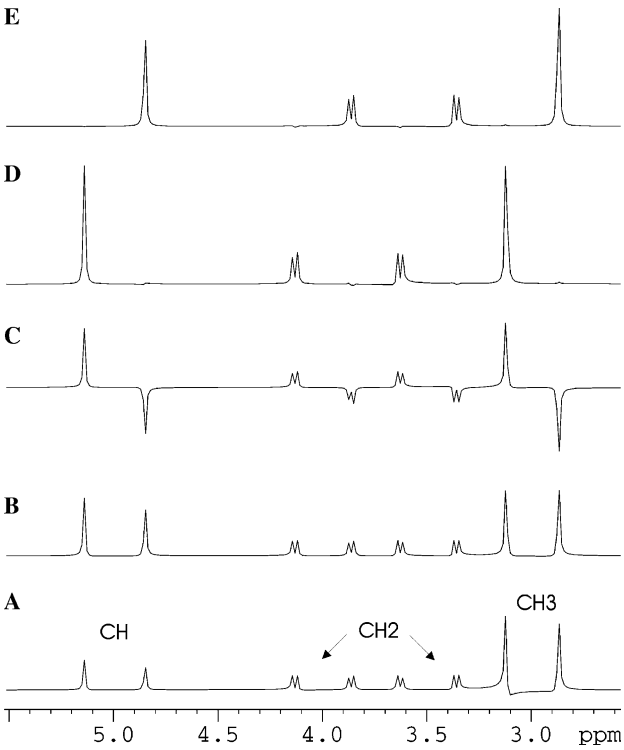

Fig. 2. Simulated 1D ^{1}H–^{13}C HSQC spectra obtained without ^{13}C decoupling during ^{1}H acquisition (see Fig. 1A) for isolated CH ($J_{CH} = 145$ Hz), CH_2 ($J_{CH} = 135$ Hz, $J_{H_1H_2} = 10$ Hz), and CH_3 ($J_{CH} = 125$ Hz) spin systems. All inter-pulse delays were optimized to an average value of 135 Hz ($\Delta = \Delta_1 = \Delta_2 = 1/2J = 3.7$ ms). (A) Conventional 1D HSQC without the PEP approach; (B) 1D HSQC-IP(y); (C) 1D HSQC-AP(y); (D–E) Addition and subtraction of IP and AP spectra afford spin-state-selective HSQC-IPAP-α/β spectra for all multiplicities. All one-dimensional spectra are drawn with the same relative intensity scale.

(point c in Fig. 1). The major drawback of this approach is that only half of the available magnetization becomes observable (Tables 1–3). In this approach the percentage of undesired cross-talk should be defined by $\frac{I_{sub}}{I_{add}} = \frac{1-s}{1+s}$, the overall sensitivity of the experiment depends only on $\sin(\pi J_{IS}\Delta)$ and is independent of the multiplicity. As mentioned previously, the incorporation of the PEP concept in combination with gradient echoes into the HSQC pulse scheme (see mixing sequence in Fig. 1B) provides sensitivity enhancement as a function of the inter-pulse delay Δ_1 settings. The expected signal-to-noise enhancements of the PEP approach (HSQC-IP(y) experiment) are well established in terms of delay optimization and I_nS multiplicity, as summarized in line 1 of Table 4 [2]. This Table 4 also contains the analysis of the remaining three experiments proposed here with the corresponding amplitude transfer functions.

In order to evaluate performance of the new experiments, the corresponding COS-CT $2I_zS^- \rightarrow I^-$ HSQC-IP and COS-CT $2I_zS^- \rightarrow 2I^-S_z$ HSQC-AP spectra were simulated using the 1D pulse sequence of Fig. 1A and the effects on different I_nS multiplicities as a function of the delays (Δ_1 and Δ_2) were analyzed (Fig. 2). A realistic case consisting of an isolated methine CH group, with a $^1J_{CH}$ of 145 Hz, a diastereotopic CH_2 methylene spin system, with a $^1J_{CH}$ of 135 Hz and a geminal $^2J_{H_1H_2}$ value of 10 Hz, and a methyl CH_3 group with a $^1J_{CH}$ of 125 Hz was considered. As can be appreciated from Figs. 2D and E, separate co-addition and subtraction of these IP and AP data afford a general approach to achieve COS-CT $2I_zS^- \rightarrow 2I^-S^{\alpha/\beta}$ for all I_nS multiplicities. Transfer efficiencies for each multiplicity follow the theoretical predictions (Fig. 3). Thus, for a IS spin system, the addition (or subtraction) of the two spectra increases the signal intensity by a factor of 2 while the noise is increased only by a square root of 2, thus resulting in S/N being increased by the square root of 2. It is also deduced that the overall sensitivity, the gain factor, and the Δ_1 delay optimization associated to each I_nS multiplicity in the HSQC-AP(y) experiment (Fig. 3B) show similar trends as already known for the HSQC-IP(y) experiment (Fig. 3A): Ideally, Δ_2 must be always set to $1/2J$ in both experiments and IS systems reach out the maximum amplitude transfer for $\Delta_1 = 1/2J$ whereas I_2S and I_3S offer maximum sensitivity at $\Delta_1 = 1/4J$ and $\Delta_1 = 1/6J$, respectively.

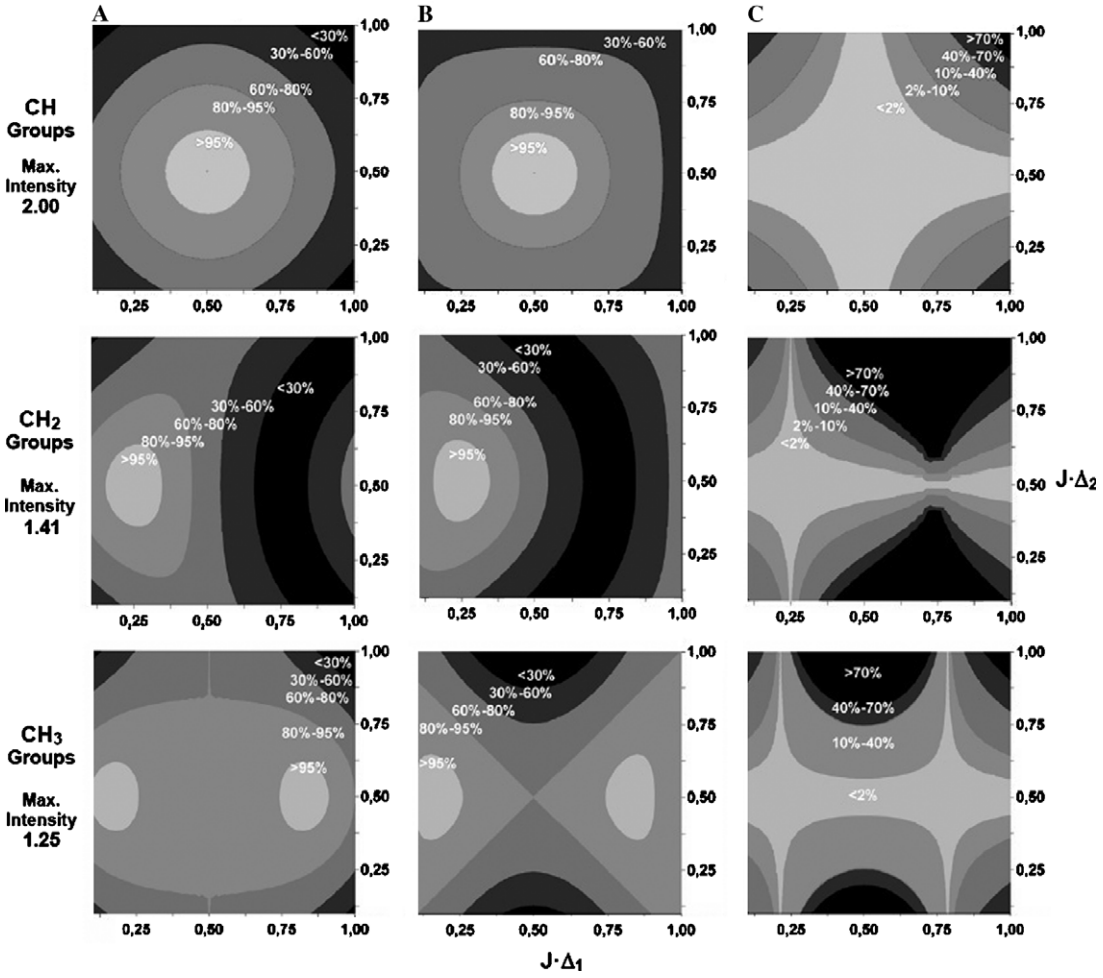

Fig. 3. Theoretical transfer efficiency as a function of the Δ_1 (x-axis) and Δ_2 (y-axis) delays for each IS, I_2S and I_3S multiplicity in the (A) HSQC-IP(y) and (B) HSQC-AP(y) experiments, and (C) cross-talk percentage in the resulting HSQC-IPAP(y) experiment. The transfer efficiency represents the percentage of the maximum signal intensity described in Table 4.

The cross-talk in the resulting HSQC-IPAP(y) experiment is defined by

$$\frac{I_{\mathrm{sub}}}{I_{\mathrm{add}}} = \frac{(c^{n-1} - s)(s' - 1)}{(c^{n-1} + s)(s' + 1)}.$$

As a consequence, the theoretical percentage of cross-talk is independent of the delay Δ_1 if Δ_2 exactly match $1/2J_{\mathrm{IS}}$ (Fig. 3C). Therefore, the Δ_1 delay optimization only affects the relative intensity deviation of each IS, I_2S, and I_3S groups from their theoretical maxima. As could be deduced from the simulations (Fig. 3C), the percentage of cross-talk is below 2.5% for all multiplicities in a J interval around ± 15 Hz. The diastereotopic CH_2 spin system should be the most sensitive multiplicity to cross-talk effects. For instance, in the case of ^1H–^{13}C experiments, by optimizing both Δ_1 and Δ_2 delays to $1/2J_{\mathrm{CH}}$ (3.6 ms for $J_{\mathrm{CH}} = 140$ Hz), the relative intensities (and cross-talk percentage) for CH, CH_2, and CH_3 groups with $J_{\mathrm{CH}} = 125$ Hz are 1.976 (0.01%), 1.14 (0.90%), and 1.01 (1.19%), respectively, whereas for $J_{\mathrm{CH}} = 155$ Hz are 1.967 (0.01%), 0.80 (2.45%), and 1.02 (1.57%), respectively. If Δ_1 is optimized to $1/4J_{\mathrm{CH}}$ for maximizing CH_2 signal intensities (1.8 ms for $J_{\mathrm{CH}} = 140$ Hz), the relatives intensities are 1.64 (0.26%), 1.40 (0.10%), and 1.22 (0.67%) for $J_{\mathrm{CH}} = 125$ Hz and 1.75 (0.22%), 1.40 (0.15%), and 1.17 (0.51%) for $J_{\mathrm{CH}} = 155$ Hz. The simulated spectra of Fig. 4 clearly show the main advantages of our approach compared to the original HSQC-α/β experiment: Improved sensitivity and optimum spin-editing are achieved for all multiplicities in the same experiment. Unfortunately, stronger J deviations around ± 30 Hz would affect the relative intensity and the cross-talk percentage (>5–6%) in a major extent for all multiplicities.

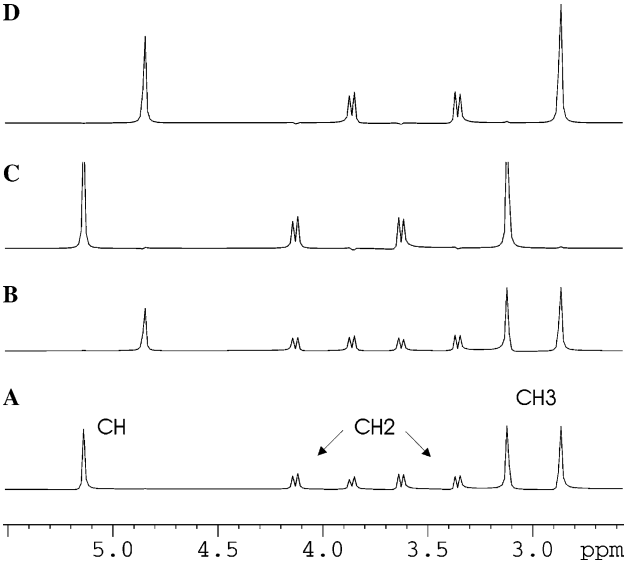

Fig. 4. Comparison of the theoretical sensitivity and spin-editing capabilities for different CH, CH_2, and CH_3 spin systems between (A and B) the original HSQC-α/β experiment [3] and (C and D) the HSQC-IPAP(y) spectra obtained with the procedure outlined here. All inter-pulse delays were optimized to an average value of 135 Hz ($\Delta = \Delta_1 = \Delta_2 = 1/2J = 3.7$ ms). See caption of Fig. 2 for more details of the simulations.

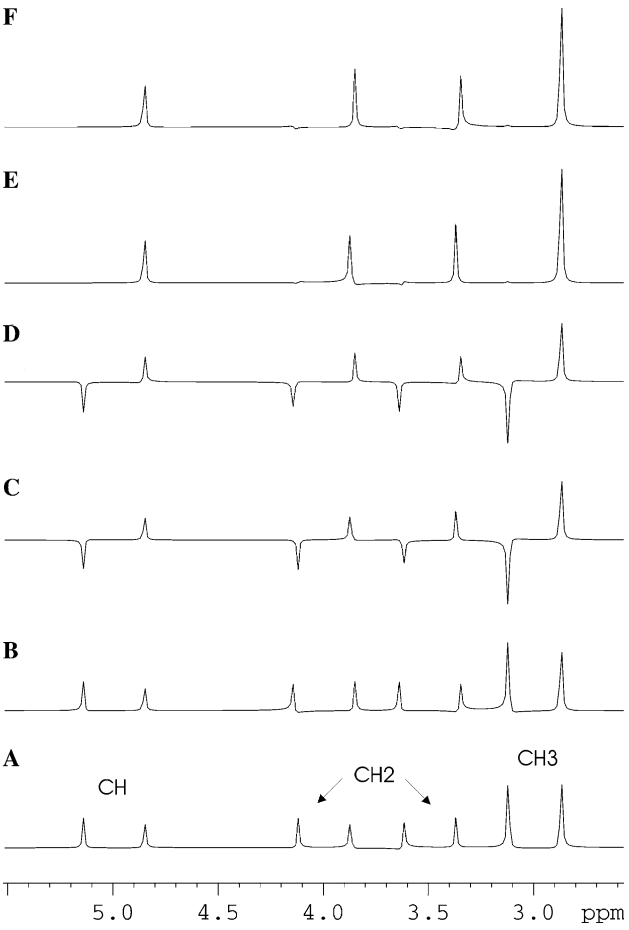

Fig. 5. Comparison of the theoretical sensitivity ratios and spin-editing capabilities for different CH, CH_2, and CH_3 spin systems in the HSQC-IP(x) experiment. (A and B) HSQC-IP(x) and HSQC-IP($-x$) that show the same ZQ (the splitting is defined by $^1J_{\mathrm{CH}}$–$^2J_{\mathrm{HH}}$) and DQ (the splitting is defined by $^1J_{\mathrm{CH}}$–$^2J_{\mathrm{HH}}$) coupling patterns and relative sensitivity for the CH_2 spin system (diastereotopic protons appearing at 4.0 and 3.5 ppm) as the conventional CH_2-optimized HSQC-α/β experiment [11]; (C and D) HSQC-AP(x) and HSQC-AP($-x$) showing anti-phase ZQ and DQ patterns for the CH_2 groups in addition to the anti-phase multiplets with respect to ^1J(CH) for CH and CH_3 groups; (E and F) Representative HSQC-IPAP(x) and HSQC-IPAP($-x$) spectra after addition of A + C and B + D, respectively.

Alternatively, another way of spin selection in I_2S spin systems can be obtained by setting $\Psi = x$ (HSQC-IP(x) experiment) (see third line in Tables 1–3). As similarly reported in [24], a double-quantum (DQ) multiplet pattern displaying only the inner lines is obtained for each diastereotopic proton (Fig. 5A). The separation between these lines equals to ^1J(CH) + ^2J(HH). On the other hand, an equivalent HSQC-IP($-x$) experiment ($\Psi = -x$) yields a zero-quantum (ZQ) pattern in which only the outer lines are obtained (Fig. 5B), representing the ^1J(CH) – ^2J(HH) value. In fact, as shown from the amplitude transfer factors of Table 4, the second retro-INEPT Δ_2 period is not necessary in the HSQC-IP(x) or ($-x$) experiment. Thus, although the sequence is a little longer than the original experiment (Fig. 1C), all the advantages on I_2S spin systems are fully retained: (i) all magnetization components

are observable and therefore, signal intensity is maximized (see line 3 in Table 4); (ii) the inter-pulse Δ_1 delay can be specifically optimized for methylene systems ($=1/2J$); (iii) the experiment allows the simultaneous measurement of the sign and the magnitude of geminal ^2J(HH) and ^1J(IS) using the described DQ–ZQ methodology (Figs. 5A and B); (iv) these IP data can be combined accordingly with the corresponding HSQC-AP(x) and HSQC-AP($-x$) data. These fully complementary AP data are obtained by exchanging ϕ_2 and ϕ_3 in both HSQC-IP(x) and HSQC-IP($-x$) experiments; and (v) editing for all other multiplicities is also feasible in the same spectra. The theoretical transfer efficiencies in the HSQC-IP(x) and HSQC-AP(x) experiments for each I_nS multiplicity are represented in Figs. 6A and B and the corresponding simulated 1D HSQC-AP(x) and HSQC-AP($-x$) spectra are shown in Figs. 5C and D, respectively. The same post-acquisition addition/subtraction procedure described above affords sensitivity-improved multiplet-selective line editing for I_2S spin systems (see Figs. 5E and F and multiplet expansions in Fig. 7), equivalent to a COS $2I_{1z}S^- \rightarrow 2I_1^-I_2^{\alpha/\beta}S^{\alpha/\beta}$ transfer, whereas heteronuclear S^3 editing is also achieved for IS and I_3S groups (Figs. 5E and F). Thus, a different and complete homonuclear and heteronuclear spin-editing in CH_2 systems is possible after combination of four spectra (Fig. 7). Although half of signal is lost for IS spin system compared to the HSQC(y) experiment, this can be a price to be paid for the additional information provided in this version.

The cross-talk in HSQC-IPAP(x) experiment, defined by

$$\frac{I_{\text{sub}}}{I_{\text{add}}} = \frac{1-s}{1+s},$$

is independent of the multiplicity (Fig. 6C). As an example, optimizing a ^{1}H–^{13}C HSQC(x) experiment to $J_{CH} = 140$ Hz (both Δ_1 and Δ_2 delays at $1/2J = 3.6$ ms) the relative intensities (and cross-talk percentages) are 0.99 (1.25%), 1.97 (1.25%), and 1.29 (1.25%) for CH, CH_2, and CH_3 groups, whereas for $J = 155$ Hz they are 0.98 (1.68%), 1.97 (1.68%), and 0.62 (1.68%).

In order to test the above theoretical predictions, the performance of the proposed IPAP principle was tested on a standard sample of menthol because it contains several CH, CH_2, and CH_3 spin systems. Fig. 8 clearly distinguishes the spin coupling pattern obtained for each multiplicity in the conventional HSQC-α/β and in our HSQC-IPAP(y) subspectra. As expected, the analysis of relative sensitivities and spin-editing features for some selected 1D slices (Fig. 9) confirms the theoretical results. Thus, whereas the spectrum shown in Fig. 9B was acquired

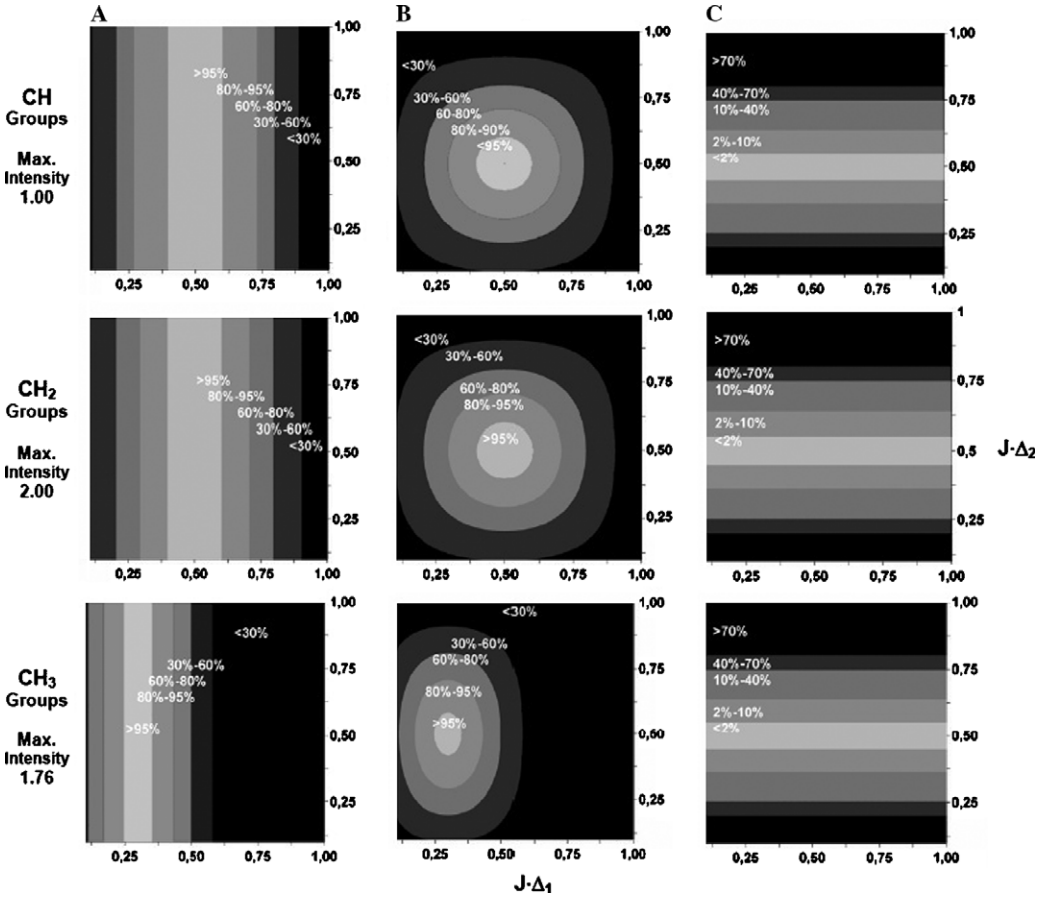

Fig. 6. Theoretical transfer efficiency as a function of the Δ_1 and Δ_2 delays for each IS, I_2S, and I_3S multiplicity in the (A) HSQC-IP(x) and (B) HSQC-AP(x) experiments, and (C) cross-talk percentage in the resulting HSQC-IPAP(x) experiment. The transfer efficiency represents the percentage of the maximum signal intensity described in Table 4.

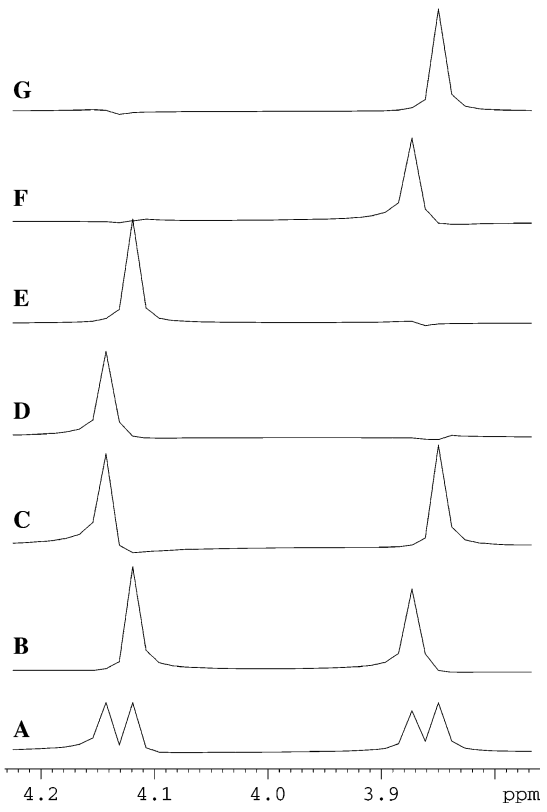

Fig. 7. Spin-editing features of a proton belonging to a diastereotopic CH_2 spin system in the HSQC-IPAP(x) experiment. (B and C) The HSQC-IP(x) and HSQC-IP($-x$) experiment showing the ZQ and DQ coupling pattern, respectively; (D–G) The four lines can be individually selected by proper combination of the following four spectra: HSQC-IP with $\Psi = x$ and $-x$, and HSQC-AP with $\Psi = x$ and $-x$.

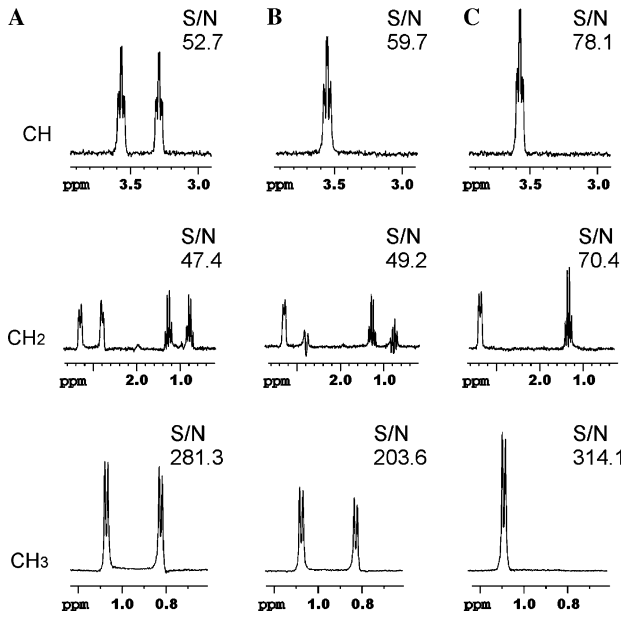

Fig. 9. Experimental 1D slices at 71.8 (CH), 45.4 (CH_2), and 21.4 (CH_3) extracted from the (A) 2D HSQC-IP(y) acquired with four scans, (B) the original 2D HSQC-α also acquired with four scans (Fig. 8A), and (C) the 2D HSQC-IPAP(y) spectrum resulting of the addition of the two IP and AP spectra acquired with four scans each one (Fig. 8C). The experimental signal-to-noise (S/N) ratio is indicated in each case for comparison. See Section 3 for more details.

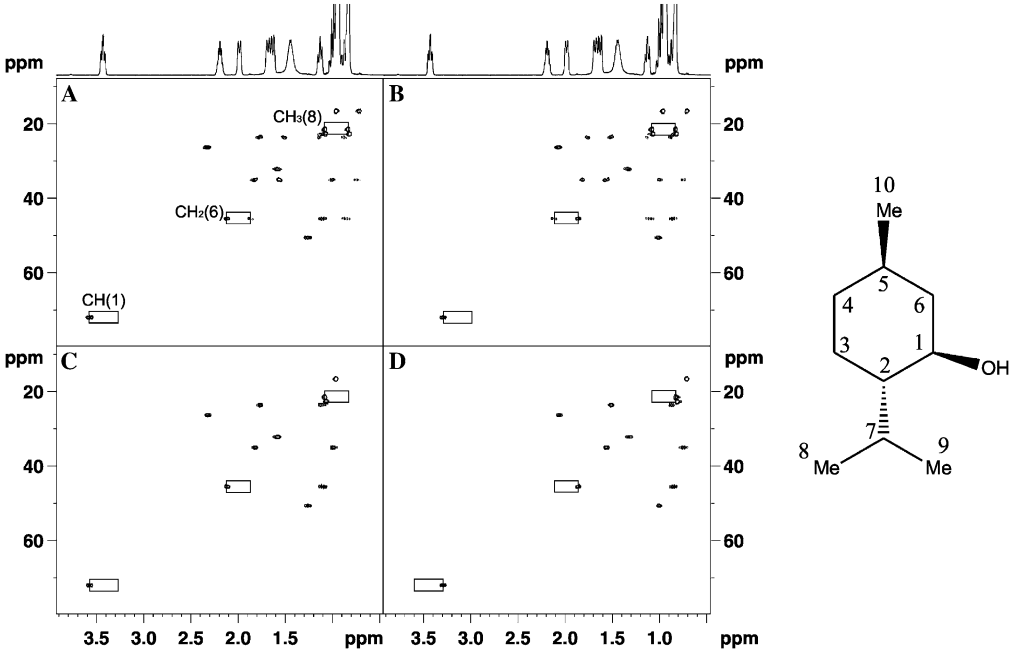

Fig. 8. 2D spin-edited HSQC-α/β spectra of menthol. (A and B) Acquired with the original pulse sequence of Fig. 1C; (C and D) 2D HSQC-IPAP(y) spectra obtained after acquisition of the IP and AP data using the sequence displayed in Fig. 1B and further addition(IP + AP)/subtraction(IP − AP) as described in the main text. For simplicity, spin-editing in some selected CH, CH_2, and CH_3 cross-peaks are marked with a box. The Δ_1 and Δ_2 delays were set at $1/4J$ (1.85 ms) and $1/2J$ (3.7 ms), respectively. See Section 3 for more details.

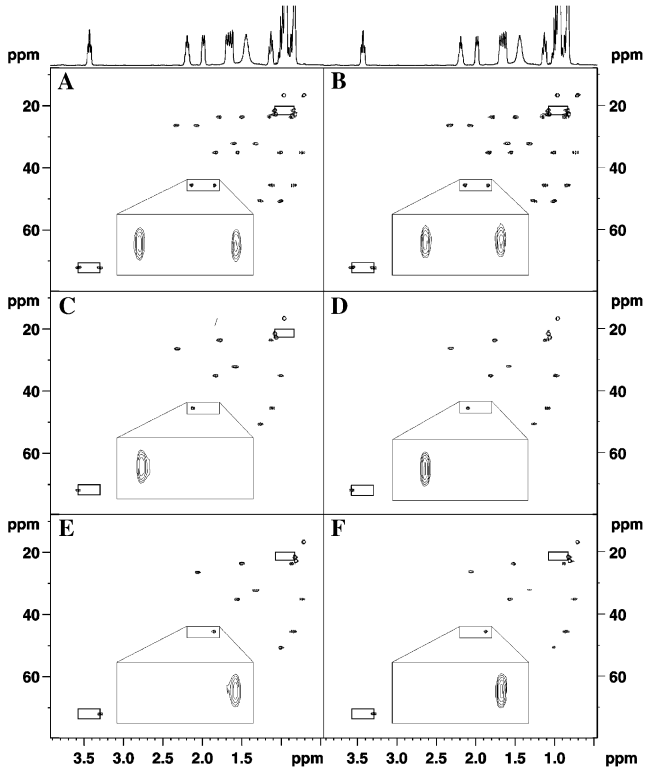

Fig. 10. 2D spin-edited HSQC(x) spectra of menthol with expanded boxes to show the spin-editing for a diastereotopic proton belonging to a CH_2 spin system: (A) 2D HSQC-IP(x) showing DQ splitting for CH_2 resonances; (B) 2D HSQC-IP($-x$) showing ZQ splitting for CH_2 resonances; (C and E) 2D HSQC-IPAP(x) and (D and F) 2D HSQC-IPAP($-x$) obtained after addition or subtraction of the corresponding IP and AP data. Note the individual line selection for CH_2 resonances whereas heteronuclear spin selection is simultaneous achieved for CH and CH_3 groups. Both Δ_1 and Δ_2 delays were set at $1/2J$ (3.7 ms). See Section 3 for more details.

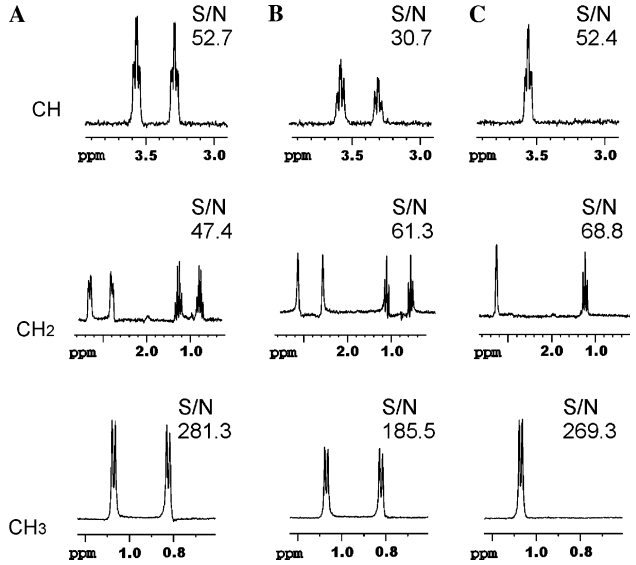

Fig. 11. Experimental 1D slices at 71.8 (CH), 45.4 (CH_2), and 21.4 (CH_3) extracted from (A) the conventional 2D HSQC-IP(y) acquired with four scans, (B) 2D HSQC-IP(x), acquired also with four scans, where the simplified ZQ pattern for the CH_2 multiplet can be observed (extracted from Fig. 10B) and (C) 2D HSQC-IPAP(x) spectrum resulting of the addition of the two IP(x) and AP(x) spectra acquired with two scans each one. The experimental signal-to-noise (S/N) ratio is indicated in each case for comparison.

with the HSQC-α/β editing method with four scans, another four scans were needed to be accumulated to obtain the second part of the doublet for the CH spin system (data not shown). This affords an unwanted sensitivity lost per time unit which is clearly observed from the same edited spectrum obtained with the addition of the IP + AP data, each one also accumulated with four scans (Fig. 9C). In addition, clean editing and improved sensitivity is also achieved for the CH and CH_3 groups. Similar conclusions can be extracted after careful examination of the corresponding HSQC(x) subspectra (Fig. 10) and some corresponding 1D traces (Fig. 11). In order to compare the overall sensitivity of the different approaches presented here we have used a sensitivity-per-time factor for CH_2 groups that can be defined as the signal-to-noise ratio obtained for each multiplet with respect to the required time needed to acquire all line multiplets. Thus, in analogy with Fig. 9, it has been necessary to accumulate two data with four scans to achieve the separate DQ and ZQ spectra (Fig. 11B) whereas to obtain line-selective editing for CH_2 spin systems four different data with two scans each one are needed. The corresponding slices in Fig. 11B belong to a HSQC-IP(x) spectrum acquired with four scans whereas Fig. 11C show the resulting spectra after addition of HSQC-IP(x) and HSQC-AP(x) data acquired with two scans each one (the other possible three combinations are not shown but display similar signal-to-noise ratios). In the traces of Fig. 11C, the clean spin-editing for CH and CH_3 spin systems combined with the line-selective spin-editing for CH_2 groups (DQ or ZQ) is clearly illustrated and a direct comparison with the traces from Fig. 9C confirms that all experimental signal-to-noise values are in good agreement with the expected enhancements.

To illustrate a useful application of the IPAP method proposed here, all long-range proton–carbon coupling constants ($^nJ_{CH}$, $n > 1$) of menthol were measured from a F2-coupled sensitivity-improved HSQC-TOCSY-IPAP experiment [29]. The excerpt of Fig. 12 shows that the sign and the magnitude of $^nJ_{CH}$ can be accurately extracted for all CH, CH_2, and CH_3 carbons with optimum sensitivity compared to the original spin-edited HSQC-TOCSY experiment, which is strongly limited only to CH spin systems [22,23].

It is worth to mention that the proposed IPAP approach shows excellent tolerance to the presence of cross-talk and takes advantage of the high digital resolution in the acquisition dimension and the high sensitivity related to the HSQC experiment. However, it is also recognized that the major inconvenient to measure J from the directly detected F2 dimension is the possible presence of strong coupling and other line distortion effects, that could afford asymmetric multiplets that make the accurate measurement more difficult. The idea can be successfully applied to achieve spin-editing for both

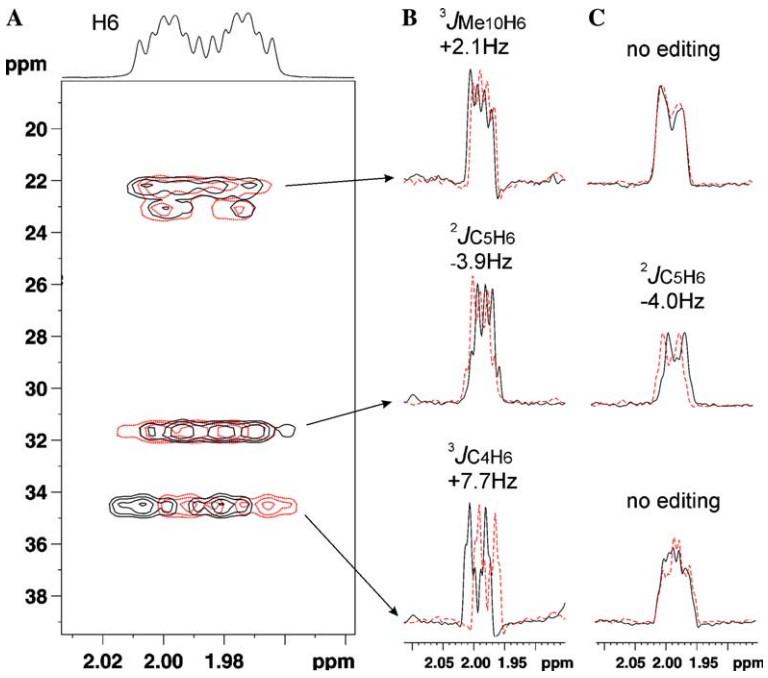

Fig. 12. (A) Expansion region of the 2D F2-spin-edited HSQC-TOCSY-IPAP experiment showing several relayed correlations involving the methylene H6 proton of menthol. (B and C) 1D slices for the methine C5, methylene C4, and methyl C10 carbons extracted from the (B) IPAP experiment and (C) the original spin-edited HSQC-TOCSY experiment [22].

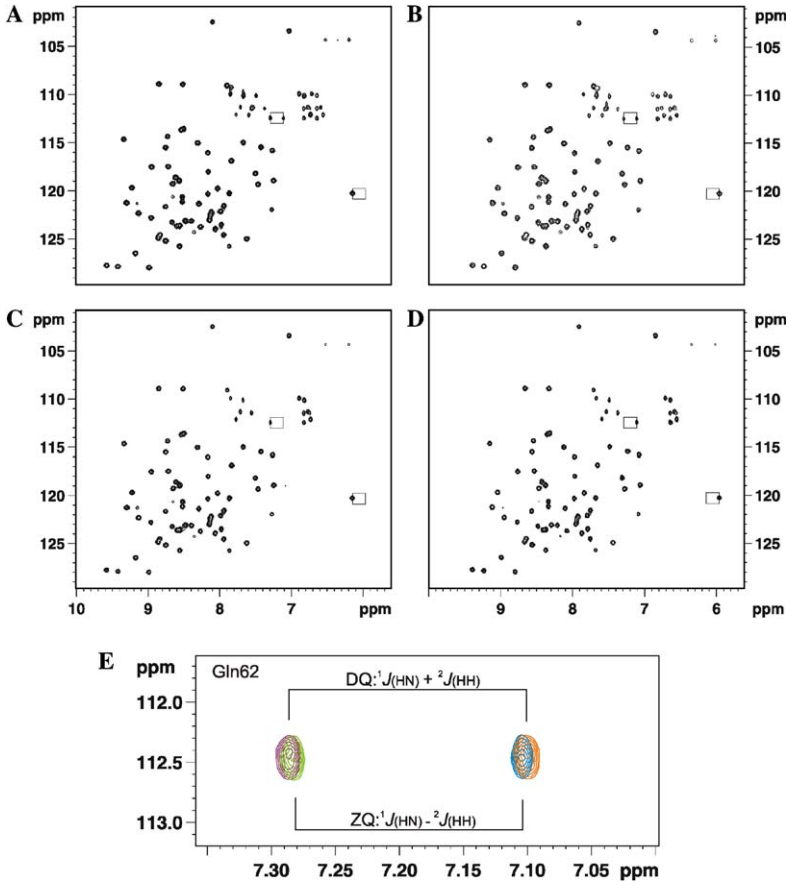

Fig. 13. 2D spin-edited ^1H–^{15}N HSQC-IPAP spectra of ubiquitin. Spin-editing for a target NH and NH_2 resonance is marked with a box in the (A and B) HSQC-α/β and the (C and D) HSQC-IPAP(y) spectra. (E) Individual spin-edited DQ/ZQ multiplet patterns in NH_2 protons obtained after proper combination of separate HSQC-IP(x, $-x$) and HSQC-AP(x, $-x$) experiments.

NH and NH_2 spin systems in isotopic labeled proteins (Fig. 13) and also easily applied in more sophisticated triple-resonance multidimensional NMR experiment in which the sensitivity-enhanced block is usually inserted prior to acquisition. However, cross-correlation effects could be affect expected signal intensities in large biomolecules and a more detailed and comparative study of relaxation properties between in-phase and anti-phase magnetization components is under study.

3. Experimental part

All experimental 2D spectra reported in this paper were recorded on a Bruker Avance500 spectrometer operating at 500.13 MHz for ^1H at 298 K. ^1H–^{13}C experiments were recorded on a 5 mm TXI probe using a sample of 20 mg of menthol dissolved in 600 μl of $CDCl_3$. If otherwise indicated, each HSQC experiment used a pre-scan delay of 1 s and four scans for each t_1 increment, with an overall experimental time of 11 min for each 2D spectrum. All inter-pulse delays were optimized to 135 Hz: The Δ and Δ_2 delays were always set at $1/2J$ (3.7 ms), whereas Δ_1 was set to $1/4J$ (1.85 ms) in Figs. 8 and 9 and to $1/2J$ (3.7 ms) in Figs. 10 and 11. The same acquisition and processing conditions were used for the 2D HSQC-TOCSY experiment of Fig. 12, only changing the number of scans to 16 and incorporating a 7 kHz DIPSI-2 multiple pulse TOCSY scheme with a duration of 35 ms. The experimental time was of 32 min. In all ^{13}C experiments discussed here, all 180° ^{13}C pulses could be replaced by adiabatic pulses if necessary for a good inversion/refocusing.

Spin-edited ^1H–^{15}N HSQC experiments were recorded on a 5 mm TCI $^1H/^{13}C/^{15}N$ cryoprobe using a 1 mM sample of doubly labeled ubiquitin sample dissolved in 90% H_2O/10% D_2O. The same pulse sequences of Figs. 1B and C were used but applying a purgue gradient pulse during the *zz* filter. Experimental conditions to record ^1H–^{15}N HSQC spectra of Fig. 13 were: 1 s of pre-scan delay and four scans for each t_1 increment. All inter-pulse delays were optimized to 90 Hz: The Δ and Δ_2 delays were set at $1/2J$ (2.77 ms) whereas Δ_1 was set to $1/4J$ (1.39 ms). Total experimental time for each 2D spectrum was of 10 min.

All 2D HSQC spectra were acquired with 128 t_1 increments and with 1K data points in the acquisition dimension. Phase-sensitivity data were obtained for all 2D experiments using the conventional gradient-based echo–antiecho protocol for data acquisition and data processing (see Figs. 1B and C). The phase Ψ was incremented by 180° together with the de-phasing gradient G1. A gradient ratio of 4:1 (for ^{13}C experiments) and 10:1 (for ^{15}N experiments) was used and gradients were 1 ms long. Data were processed using a zero-filling up to 256 and a cosine window was applied in both t_1 and t_2 dimensions prior to Fourier transformation. In the IPAP approach, IP and AP data were separately recorded and stored, and further processed (added or subtracted) before Fourier transformation.

Calculated 1D spectra were simulated using the program NMRSIM (Bruker AG) using the pulse sequence of Fig. 1A. All 1D fully coupled ^1H proton spectra were simulated with a 2:−2:1 gradient ratio and with experimental details described in the corresponding figure captions.

4. Conclusions

A versatile spin-state selection approach for all multiplicities in the HSQC experiment has been introduced, combining optimized sensitivity and minimal undesired cross-talk. Methylene-specific multiplet-line selection can also be achieved with maximum sensitivity whereas spin selection for all other multiplicities is retained. It can be anticipated that this novel methodology can have an important impact in the simultaneous measurement of the magnitude and the sign of homonuclear and heteronuclear scalar and/or residual dipolar coupling constants from the same spectra. Different multidimensional NMR experiments could be also benefit of the proposed approach. We are currently investigating this application to experiments designed for the measurement of heteronuclear coupling constants involved in both backbone (NH and CH) and side-chain (CH_2, CH_3, and NH_2) frameworks in labeled proteins.

Acknowledgments

This work was supported by MCYT (Project BQU2003-01677) and Centro de Investigación Lilly. We are also grateful to the Servei de Ressonància Magnètica Nuclear, UAB, for allocating instrument time to this project and to Bruker Española S.A. for its continuing support. P.N. thanks ''Generalitat de Catalunya'' for a predoctoral grant.

References

[1] L.E. Kay, P. Keifer, T. Saarinen, Pure absorption gradient-enhanced heteronuclear single-quantum correlation spectroscopy with improved sensitivity, J. Am. Chem. Soc. 114 (1992) 10663–10665.
[2] J. Schleucher, M. Schwendinger, M. Sattler, P. Schmidt, O. Schedletzky, S.J. Glaser, O.W. Sorensen, C. Griesinger, A general enhancement scheme in heteronuclear multidimensional NMR employing pulsed field gradients, J. Biomol. NMR 4 (1994) 301–306.
[3] K. Pervushin, R. Riek, G. Wider, K. Wüthrich, Attenuated T2 relaxation by mutual cancellation of dipole–dipole coupling and chemical shift anisotropy indicates an avenue to NMR structures of very large biological macromolecules in solution, Proc. Natl. Acad. Sci. USA 94 (1997) 12366–12371.
[4] M.D. Sorensen, A. Meissner, O.W. Sorensen, Spin-state-selective coherence transfer via intermediate states of two-spin coherence in IS spin systems. Application to E.COSY-type measurement of *J* coupling constants, J. Biomol. NMR 10 (1997) 181–186.
[5] A. Meissner, J.O. Duus, O.W. Sorensen, Integration of spin-state-selective excitation into 2D NMR correlation experiments with heteronuclear ZQ/DQ π rotations for ^1J(XH)-resolved E.COSY-type measurement of heteronuclear coupling constants in proteins, J. Biomol. NMR 10 (1997) 89–94.
[6] P. Andersson, J. Weigelt, G. Otting, Spin-state selection filters for the measurement of heteronuclear one-bond coupling constants, J. Biomol. NMR 12 (1998) 435–441.

[7] M.D. Sorensen, A. Meissner, O.W. Sorensen, ^{13}C natural abundance S^3E and S^3CT experiments for measurement of J coupling constants between $^{13}C^{\alpha}$ or $^{1}H^{\alpha}$ and other protons in a protein, J. Magn. Reson. 137 (1999) 237–242.

[8] M. Ottiger, F. Delaglio, A. Bax, Measurement of J and dipolar couplings from simplified two-dimensional NMR spectra, J. Magn. Reson. 131 (1998) 373–378.

[9] D. Yang, L.E. Kay, Improved NH-detected triple-resonance TROSY-based experiments, J. Biomol. NMR 13 (1999) 3–10.

[10] D. Nietlispach, Suppression of anti-TROSY lines in a sensitivity enhanced gradient selection TROSY scheme, J. Biomol. NMR 31 (2005) 161–166.

[11] M. Sattler, J. Schleucher, O. Schedletzky, S.J. Glaser, C. Griesinger, N.C. Nielsen, O.W. Sorensen, a&b HSQC, an HSQC-type experiment with improved resolution for I_2S groups, J. Magn. Reson. A 119 (1996) 171–179.

[12] T.S. Untidt, T. Schulte-Herbruggen, O.W. Sorensen, N.C. Nielsen, Nuclear Magnetic Resonance coherence-order and spin-state-selective correlation in I_2S spin systems, J. Phys. Chem. A 103 (1999) 8921–8926.

[13] E. Miclet, E. O'Neil-Cabello, E.P. Nikonowicz, D. Live, A. Bax, ^{1}H–^{1}H dipolar couplings provide a unique probe of RNA backbone structure, J. Am. Chem. Soc. 125 (2003) 15740–15741.

[14] E. Miclet, J. Boisbouvier, A. Bax, Measurement of eight scalar and dipolar couplings for methine–methylene pairs in proteins and nucleic acids, J. Biomol. NMR 31 (2005) 201–216.

[15] E. Miclet, D.C. Williams Jr., G.M. Clore, D.L. Bryce, J. Boisbouvier, A. Bax, Relaxation-optimized NMR spectroscopy of methylene groups in proteins and nucleic acids, J. Am. Chem. Soc. 126 (2004) 10560–10570.

[16] T. Carlomagno, W. Peti, C. Griesinger, A new method for the simultaneous measurement of magnitude and sign of $^{1}D_{CH}$ and $^{1}D_{HH}$ dipolar couplings in methylene groups, J. Biomol. NMR 17 (2000) 99–109.

[17] V. Tugarinov, P.M. Hwang, J.E. Ollerenshaw, L.E. Kay, Cross-correlated relaxation enhanced ^{1}H–^{13}C NMR spectroscopy of methyl groups in very high molecular weight proteins and protein complexes, J. Am. Chem. Soc. 125 (2003) 10420–10428.

[18] J.E. Ollerenshaw, V. Tugarinov, L.E. Kay, Methyl TROSY: explanation and experimental verification, Magn. Reson. Chem. 41 (2003) 843–862.

[19] G. Kontaxis, A. Bax, Multiplet component separation for measurement of methyl ^{13}C–^{1}H dipolar couplings in weakly aligned proteins, J. Biomol. NMR 20 (2001) 77–82.

[20] K. Pervushin, B. Vögeli, Observation of individual transitions in magnetically equivalent spin systems, J. Am. Chem. Soc. 125 (2003) 9566–9567.

[21] T. Parella, M. Gairí, Simultaneous recording of spin-state-selective NMR spectra for different I_nS spin systems, J. Am. Chem. Soc. 126 (2004) 9821–9826.

[22] W. Kozminski, Simplified multiplet pattern HSQC-TOCSY experiment for accurate determination of long-range heteronuclear coupling constants, J. Magn. Reson. 137 (1999) 408–412.

[23] T. Parella, J. Belloc, Spin-state-selective excitation in selective 1D inverse NMR experiments, J. Magn. Reson. 148 (2001) 78–87.

[24] P. Permi, A spin-state-selective experiment for measuring heteronuclear one-bond and homonuclear two-bond couplings from an HSQC-type spectrum, J. Biomol. NMR 22 (2002) 27–35.

[25] P. Permi, Two simple NMR experiments for measuring dipolar couplings in asparagines and glutamine side chains, J. Magn. Reson. 153 (2001) 267–272.

[26] K. Ding, A.M. Gronenborn, Sensitivity-enhanced E.COSY-type HSQC experiments for accurate measurements of one-bond ^{15}N–^{1}HN, ^{15}N–$^{13}C'$ and two-bond $^{13}C'$–^{1}HN residual couplings in proteins, J. Magn. Reson. 158 (2002) 173–177.

[27] D. Lee, B. Vögeli, K. Pervushin, Detection of C',C^{α} correlations in proteins using a new time- and sensitivity-optimal experiment, J. Biomol. NMR 31 (2005) 273–278.

[28] P. Würtz, K. Fredriksson, P. Permi, A set of HA-detected experiments for measuring scalar and residual dipolar coupling, J. Biomol. NMR 31 (2005) 321–330.

[29] K.E. Köver, V.J. Hruby, D. Uhrin, Sensitivity- and gradient-enhanced heteronuclear coupled/decoupled HSQC-TOCSY experiments for measuring long-range heteronuclear coupling constants, J. Magn. Reson. 129 (1997) 125–129.